Nationaal Lucht- en Ruimtevaartlaboratorium
National Aerospace Laboratory NLR

NLR-TP-2000-044

A seven-point bending test to determine the strength of the skin-stiffener interface in composite aircraft panels

J.C.F.N. van Rijn and J.F.M. Wiggenraad

Nationaal Lucht- en Ruimtevaartlaboratorium
National Aerospace Laboratory NLR

NLR-TP-2000-044

A seven-point bending test to determine the strength of the skin-stiffener interface in composite aircraft panels

J.C.F.N. van Rijn and J.F.M. Wiggenraad

This report is based on an article to be published in the proceedings of the European Conference on Composite Materials ECCM9, 4-7 June 2000, Brighton, UK.

Division: Structures and Materials
Issued: 3 February 2000
Classification of title: Unclassified

Contents

3 Tables
10 Figures

(13 pages in total)

A SEVEN-POINT BENDING TEST TO DETERMINE THE STRENGTH OF THE SKIN-STIFFENER INTERFACE IN COMPOSITE AIRCRAFT PANELS

J.C.F.N. van Rijn and J.F.M. Wiggenraad
National Aerospace Laboratory NLR, The Netherlands

Keywords: composite material, failure, skin-stiffener interface, bending test method, finite element analysis, failure criterion

ABSTRACT

In numerous panel tests it was established that, in the post-buckling regime, failure of a composite stiffened panel is often induced by the separation failure of a skin-stiffener interface. The local curvature of the skin induces peel loading at the stiffener flange that results in separation of the skin and the stiffener.

Earlier, experimental research at NLR was performed on strip specimens loaded in four-point bending. Evaluation of the results led to the conclusion that specimen failure was governed by the characteristics of the skin and was triggered by stresses concentrated at the edges of the specimen. The influence of the flange lay-up was found to be only marginal.

Based on this conclusion a reconsideration of the coupon-type test was made. A novel seven-point bending test rig was designed and manufactured. In the new test configuration, the bending deformation forced onto the specimen was such that failure of the specimen did not initiate at the edges of the specimen. The failure occurred in the adhesive layer between the flange and the skin for the specimens loaded in seven-point bending, which is in accordance with the failure location found in panels with skin-stiffener interface failure.

A failure criterion is proposed for the specimens tested in seven-point bending. Evaluating the results of the four-point bending test using the criterion for seven-point bending test a remarkable similarity between the results of both test methods was established, even though the behaviour and failure characteristics for both test methods were very different. Further research is required to clarify this finding.

The work was performed as part of the Brite Euram programme entitled “Efficient Design And Verification of Composite Structures”, CEC contract number BRPR-CT98-0611. The support of the European Commission in gratefully acknowledged.

INTRODUCTION

Composite materials have become serious candidates for primary structural components of transport aircraft because of potential weight savings. Stiffened panels may be used in these components as primary load-carrying mechanisms. In numerous panel tests it

was established that, in the post-buckling regime, failure of a composite stiffened panel is often induced by the separation failure of a skin-stiffener interface. The local curvature of the skin induces peel loading at the stiffener flange that results in separation of the skin and the stiffener. A coupon-type test method is required to investigate failure mechanisms and conduct parametric studies of the factors influencing the load carrying capability of a skin-stiffener combination, such as skin, stiffener and adhesive materials, lay-ups, geometric configurations, etc. The findings of these investigations and studies should cumulate in a failure criterion for the skin-stiffener interface. Moreover, an appropriate coupon-type test would allow for the evaluation of the effects of defects and the damage tolerance properties of a skin-stiffener combination. The modelling capabilities for these phenomena are still inadequate, and characterisation is largely depending on experimental research.

Earlier, experimental research at NLR was performed on strip specimens loaded in four-point bending or lateral tension, see Thuis and Wiggenraad (1) and Van Rijn (2). The strip specimens represented a cross section of a stiffened panel and comprised a skin and either a co-bonded blade stiffener or a co-bonded stiffener flange. Evaluation of the results led to the conclusion that specimen failure was governed by the characteristics of the skin and was triggered by stresses concentrated at the edges of the specimen. The influence of the flange lay-up was found to be only marginal.

Based on this conclusion a reconsideration of the most suitable coupon-type test was made and a new test rig was designed. An experimental programme was performed to compare the performance of the new test rig to the four-point bending test.

Firstly, the newly designed test rig is described. The experimental programme is described, followed by a presentation of the results. Subsequently, a comparison of the performance of both test methods is made. Finally, conclusions reached and recommendations for future work are presented.

TEST RIG DESIGN

Based on the conclusion of Van Rijn (2) a reconsideration of the most suitable coupon-type test was made. In a new test design, the bending deformation forced onto the specimen should be such that failure of the specimen does not initiate at the edges of the specimen. As the local curvature of the skin was anticipated to be of paramount importance, the curvature along the centre line of the specimen should be larger than at the edges.

The seven-point bending test rig that evolved is shown in **Fig 1**. The specimen is supported at five locations by 15 mm steel balls. The load is introduced at two locations along the centre line of the specimen, also by 15 mm steel balls. The dimensions of the test rig are given in **Fig 2.a**. Upon loading a three-point bending deformation is forced onto the specimen along the centre line of the specimen by the two load introduction points and the central support. The four outer supports restrict the bending deformation along the edges of the specimen, thus preventing failure initiation along the edges.

The four-point bending test rig is shown in **Fig 2.b**. The dimensions of the test rig are also shown in this figure.

EXPERIMENTAL PROGRAMME

It was established in earlier experimental programmes, see Thuis (3) and Thuis (4), that a particular panel design with relatively thick stiffener flanges was prone to stringer pop-off induced failure under compression into the post-buckling regime, while an improved design with thinner stiffener flanges was not. These panel designs were used as a test case for the adequacy of the novel seven-point bending test set-up versus the four point bending test. The specimens are flat sheets representing the panel skin with an I-stiffener bonded across the width of the specimen. The dimensions of the specimens are given in **Fig 3**. The definition of the laminates is given in **Table I**. The 0º direction is along the x-axis as shown in **Fig 3**, which is parallel with the stiffener direction. The specimen codes are given in **Table II**. The skin laminates S1 and S2 were combined with the flange laminates F1 and F2 respectively. The specimens were taken from larger panels, which were manufactured earlier but had not been tested to failure. The material for all specimens was Fibredux HTA/6376. The adhesive was FM300/M. As the specimen width was identified as a potentially important parameter in the evaluation of the four-point bending results in Van Rijn (2), the four-point bending tests were performed on specimens with a width of 25, 50 or 100 mm. The seven-point bending tests were performed on specimens with a width of 250 mm. All tests were performed in triplicate.

The tests were performed on a Wolpert spindle driven testing machine. All specimens were loaded under displacement control. The loading rate was 2 mm/min.

For all specimens the load and the crosshead displacement of the testing machine were recorded continuously. For the specimens loaded in four-point bending, the deformation of and failure initiation at the specimen edge were recorded using a video camera. For the specimens loaded in the seven-point bending rig, the failure initiation at the centre line of the specimen was recorded using a video camera. The load was displayed within the camera view. The acoustic emission of the specimen was recorded using a PAC SPARTAN acoustic emission recording system, for most specimens. The acoustic emission probe had a high-frequency characteristic.

EXPERIMENTAL RESULTS

The load-displacement curves for the specimen configurations that used the stiffener with a thick flange showed a slight change of slope, which is a change of the incremental stiffness, at the onset of failure. A 20 percent decrease in slope was chosen as an indication of failure. The load-displacement for the specimen configurations that used the stiffener with a thin flange showed a marked decrease of the load at the onset of failure.

The onset of failure was either the formation of a small but clearly noticeable delamination or complete detachment of the stiffener flange. The failure location was at the first ply (a + or – 45º ply) in the skin laminate for the specimens loaded in four-point bending, as was the case in earlier programmes. For the specimens loaded in seven-point bending the failure location was in the adhesive layer between the flange and the skin. This failure mode corresponded with the stiffener pop-off failure mode found in panel tests. The video recording showed that the onset of failure for the specimen configurations that used the stiffener with a thin flange was instantaneous. The onset of failure for the specimen configurations that used the stiffener with a thick flange loaded in four-point bending was initially only noticeable as a thin dark line on the specimen edge. As the delamination grew with increasing load, the crack became more obvious.

The acoustic emission the specimen configurations that used the stiffener with a thin flange was minor until the onset of failure, at this moment a sudden increase in acoustic emission was noticeable. For the specimen configurations that used the stiffener with a thick flange a gradual increase of the acoustic emission evolved, which at some stage became progressive. This instant coincided with the onset of failure.

The failure loads and crosshead displacements at failure for all specimens are given in **Tables III** in **Fig 4**. The failure loads (**Fig 4.a**) and the crosshead displacements at failure (**Fig 4.b**) obtained by four-point bending tests were approximately the same for the specimens with thin flanges and the specimens with the thick flanges especially for the smaller specimen widths. The failure loads (**Fig 4.a**) and the crosshead displacements at failure (**Fig 4.b**) obtained by seven-point bending tests were larger for the specimens with thin flanges than for the specimens with the thick flanges.

FINITE ELEMENT ANALYSIS

The seven-point bending tests were supported by finite element analyses. For the configurations PX1 and PX2 finite element analyses were performed using NASTRAN version 70.0. In the finite element models 4-noded quadrilateral shell elements were used. The laminates were included using PCOMP-cards. The skin and the co-bonded stringer flange were modelled as a single laminate. The eccentricity of the load path was taken into account by using an offset to place the elements on the outer skin surface, i.e. the surface to which the stiffener flange was not bonded. The flange taper was taken into account by a reduction of the extent of the stiffener flange.

The deformed shape of the finite element model for the configuration PX1 is shown in **Fig 5**. It should be noted that the co-ordinate system is such that the x-axis is parallel to the stiffener, the y-axis is perpendicular to the stiffener and the z-axis is normal to the skin. On the deformed shape the distribution of the yy-component of the curvature tensor is shown. The curvature tensor gives the rate of variation of the strain tensor through the thickness of the shell, and as such is a suitable measure for the local bending deformation of the structure.

EVALUATION OF RESULTS

Results of the four-point bending tests

In Van Rijn (2) a failure criterion was derived for the skin-stiffener interface. The experimental results used in the derivation of this criterion were obtained using four-point bending tests. As the failure mode is a crack in the 45º ply in the skin closest to the interface, the failure criterion postulates that the average in-plane normal strain perpendicular to the fibre direction and the average in-plane shear angle in the 45º layer nearest to the flange govern the initiation of a delamination. The ratio between the normal strain perpendicular to the fibre direction ε_{22} and the average in-plane shear angle γ_{12} depends on the skin laminate. A laminate analysis programme LAP (5) was used to obtain the normal strain perpendicular to the fibre direction ε_{22} and the average in-plane shear angle γ_{12} as functions of the applied moment under plane strain conditions. It was established that the ratio of the normal strain perpendicular to the fibre direction and the average in-plane shear angle $\varepsilon_{22}/\gamma_{12}$ was the same for both skin laminates S1 and S2. In **Fig 6** the shear angle at failure is given for all specimens. As can be seen, there is no significant difference in failure strain between the specimens with a thicker and a thinner flange. Moreover, the results are dependent on the specimen width, which is considered to be undesirable.

Results of the seven-point bending tests

The specimens tested in seven-point bending failed at the centre line perpendicular to the stringer in the bond layer. The deformation along this centre line is given in **Fig 7**. The deformation was calculated by finite element analysis for a load equal to the experimentally determined failure load. For the thick flange the skin deformation underneath the flange was very small and just beyond the flange the skin showed a sharp bend. For the thin flange the skin also deformed underneath the flange and beyond the flange the change in skin deformation was more gradual. The calculated total displacement of the load introduction points was comparable to the experimentally determined crosshead displacements at the onset of failure.

It can be postulated that the running loads transferred through the bond layer govern failure. The running loads transferred through the bond layer are derived from the running loads in the flange through the loads and moments equilibria, as is indicated in **Fig 8**. The deformation of the flange was obtained from finite element analyses. The flange strains and curvatures were extrapolated to the edge of the flange. These flange strains and curvatures were used as input in the laminate analysis programme LAP (5) to obtain running loads and moments. The shear load F_B and the moment M_B transferred through the bond layer at failure as calculated for the specimens tested in seven-point bending are given in **Fig 9**. The ratio between the shear load and the moment transferred through the bond layer primarily depends on the flange thickness. As an indication an ellipse shaped failure envelope is included in **Fig 9**.

Clearly, the postulated criterion should be verified with experiments on specifically designed configurations. The failure envelope is premature since only two points are available for the construction of the envelope. More experiments are needed to cover

the range for the ratio between the shear load and the moment transferred through the bond layer more fully.

Comparison of the four- and seven-point bending test results
The failure location was at the first ply (a + or – 45º ply) in the skin laminate for the specimens loaded in four-point bending, as was the case in earlier programmes. For the specimens loaded in seven-point bending the failure location was in the adhesive layer between the flange and the skin. This failure mode corresponded with the stiffener pop-off failure mode found in panel tests.

The increase in specimen flexibility, which should result from the application of thinner flanges, did show in the seven-point bending tests, but was not apparent in the four-point bending tests, as can be concluded from the crosshead displacements at failure (**Fig 4.b**).

The shear load and the moment transferred through the bond layer at failure for the 100 mm wide specimens tested in four-point bending are compared to the results for the specimens tested in seven-point bending in **Fig 10**. For the specimens loaded in four-point bending the strains and curvatures in the flange and subsequently the running loads and moments in the flange were calculated using the laminate analysis programme LAP (5). The results for the four-point bending specimens and the results for the seven-point bending specimens are remarkably close. Two conclusions are possible. Either the four-point bending specimens were close to failing in the bond layer. Or in the seven-point bending test the transfer of the out-of-plane load through the bond layer, which is not taken into account in the current criterion, has a contribution in the failure process. Possibly, an adaptation of the test rig is feasible, which eliminates the transfer of the out-of-plane load through the bond layer. The overlap of the loads and moments transferred through the bond line at failure among both test methods is unexpected, as

- the failure mode and failure location were different for both tests;
- the deformations in both tests were very different;
- the failure loads for the configurations with thick flanges tested in four-point bending were quite close to those for thin flanges, whereas the failure loads for these configurations tested in seven-point bending were different.

Further analyses are required to clarify these findings, and to establish whether the overlap was phenomenological or co-incidental. In the latter case other configurations can be used to verify experimentally the relation between both test methods.

CONCLUSIONS AND RECOMMENDATIONS

A novel seven-point bending test rig was designed and manufactured. In the new test design, the bending deformation forced onto the specimen was such that failure of the specimen did not initiate at the edges of the specimen.

The failure location was at the first ply (a + or – 45º ply) in the skin laminate for the specimens loaded in four-point bending, as was the case in earlier programmes. For the specimens loaded in seven-point bending the failure location was in the adhesive layer

between the flange and the skin. This failure mode corresponded with the stiffener pop-off failure mode found in panel tests.

A criterion established in earlier work was successfully used to bring together the four-point bending results for configurations with thick and thin stiffener flanges. It was established that the influence of the stiffener flange on the failure of the skin-stiffener interface, when tested in four-point bending, is negligible. Moreover, the results are dependent on the specimen width, which is considered to be undesirable.

As the specimens tested in seven-point bending failed at the centre line perpendicular to the stringer in the bond layer, the running loads transferred through the bond layer can be postulated to govern failure. As an indication ellipse shaped failure envelopes were included.
The shear load and the moment transferred through the bond layer at failure for the four-point bending specimens are remarkably close to the results for the seven-point bending specimens.

Clearly, the postulated criterion should be verified with experiments on specifically designed configurations. The failure envelope is premature since only two points are available for the construction of the envelope. More experiments are needed to cover the range for the ratio between the shear load and the moment transferred through the bond layer more fully. Moreover, further analyses are required to clarify the relation between the four- and seven-point bending test, and to establish whether the overlap in the results was phenomenological or co-incidental.

ACKNOWLEDGEMENTS

The work was performed as part of the Brite Euram programme entitled “Efficient Design And Verification of Composite Structures”, under CEC contract number BRPR-CT98-0611. The support of the European Commission in gratefully acknowledged.

The contribution of the following co-workers is acknowledged: L. Ubels, N. de Graaf, F. Hoekstra, J. Platenkamp, and K. Mossel.

REFERENCES

1 Thuis, H.G.S.J., Wiggenraad, J.F.M., ‘Investigation of the bond strength of a discrete skin-stiffener interface’, National Aerospace Laboratory NLR technical publication TP 92183 L, 1992
2 Rijn, J.C.F.N. van, ‘Failure criterion for the skin-stiffener interface in composite aircraft panels’, National Aerospace Laboratory NLR technical publication TP 98264, July 1998
3 Thuis, H.G.S.J., ‘The design, fabrication and testing of composite intermediate (2000 N/mm) I-stiffened compression panels - VTP-composite wing box –’, National Aerospace Laboratory NLR Contract Report CR 94321 C, June 1994

4 Thuis, H.G.S.J., 'The development of a damage tolerant intermediate (2000 N/mm) composite compression panels – VTP wing box –', National Aerospace Laboratory NLR Contract Report CR 95143 C, March 1995
5 LAP, 'Laminate Analysis Programme, User Guide', Anaglyph Ltd, London, 1996

Table I Definition of the laminates

Laminate code	Laminate content (# 0º, # 45º, # 90º)	Thickness [mm]	Laminate definition
S1	(2, 12, 2)	2.9	$[\pm 45, 0, 45, 90, -45, \pm 45]_s$
S2	(4, 12, 2)	3.3	$[\pm 45, 0, \pm 45, 90, 0, \pm 45]_s$
F1	(20, 8, 2)	5.4	$[45, 0_3, -45, 0_2, 90, 0_2, -45, 0_3, 45]_s$
F2	(4, 4, 1)	1.6	$[\pm 45, 0_2, 90, 0_2, \pm 45]$

Note: the 0º direction is the direction of the stiffener axis

Table II Specimen codes

Skin laminate	Flange laminate	Specimen width			
		Four-point bending			Seven-point bending
		25 mm	50 mm	100 mm	250 mm
S1	F1	PS1	PM1	PW1	PX1
S2	F2	PS2	PM2	PW2	PX2

Table III Failure loads in [N] and crosshead displacements at failure in [mm]

	PS1	PS2	PM1	PM2	PW1	PW2	PX1	PX2
Failure load [N]	526	842	1230	1565	2629	3859	3196	5500
	616	535	1211	1471	2632	3417	3499	6329
	568	648	1197	1996	2697	4530	3744	6081
Crosshead displacement [mm]	5.87	6.53	5.63	5.47	5.74	6.36	3.22	4.34
	6.45	4.74	5.59	5.27	5.78	5.55	3.49	4.93
	6.52	5.01	5.62	7.27	5.98	7.18	3.75	4.78

Fig 1 Seven-point bending test rig

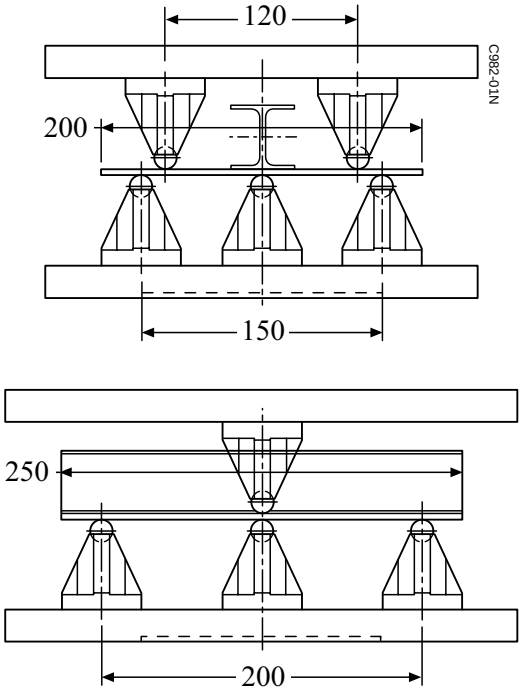

a) Seven point bending test rig

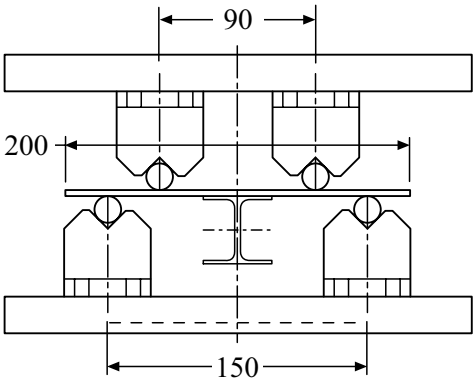

b) Four point bending test rig

Fig 2 Dimensions of bending test rig

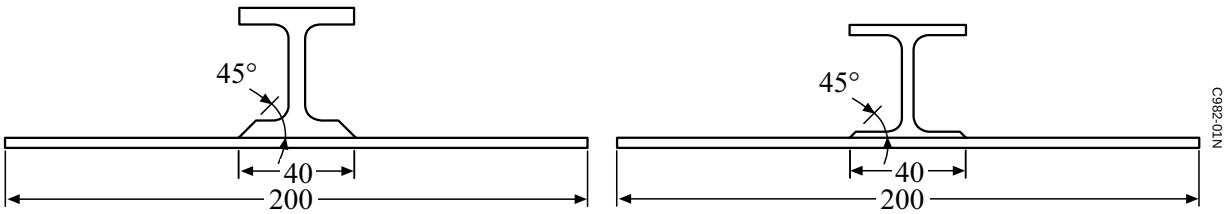

a) Specimen configuration with thick flange

b) Specimen configuration with thin flange

Fig 3 Specimen dimensions

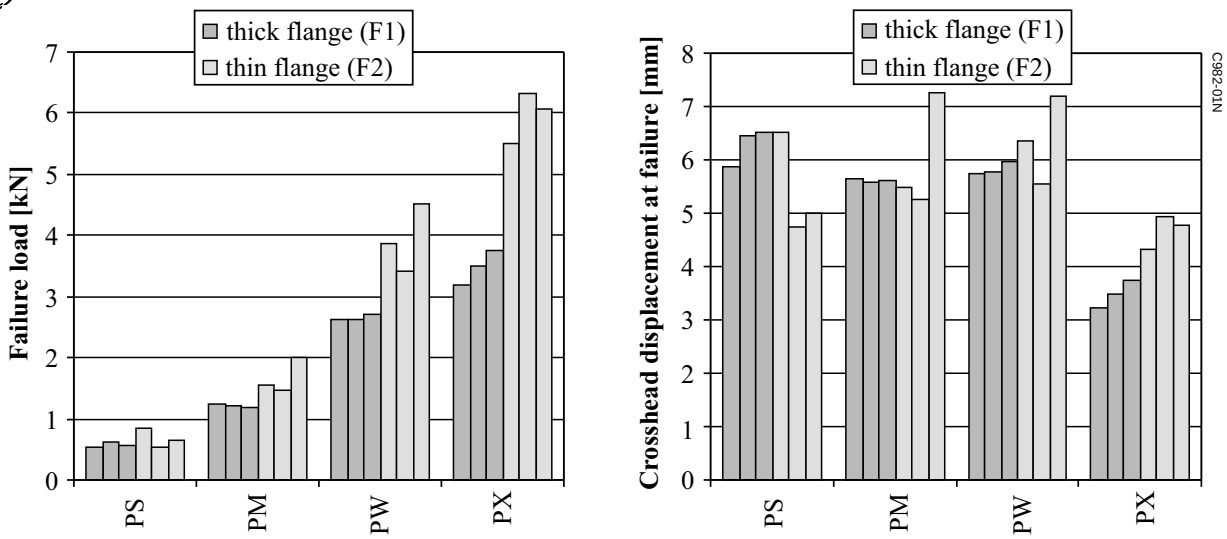

a) Failure loads b) Crosshead displacements at failure

Fig 4 Experiments results for all specimens

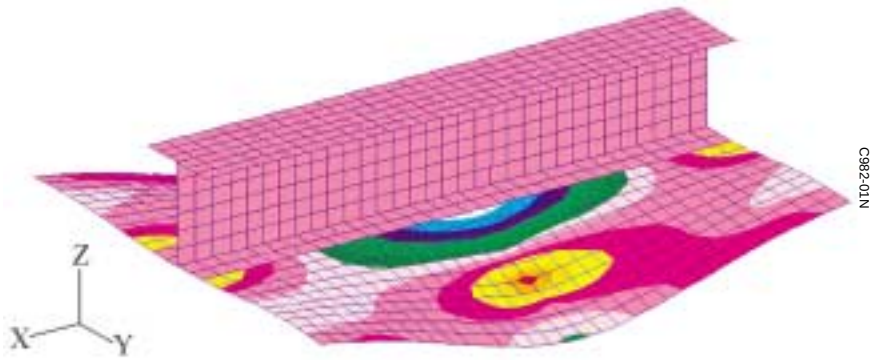

Fig 5 Deformed shape of finite element model for configuration PXI with distribution of yy-component of the curvature tensor

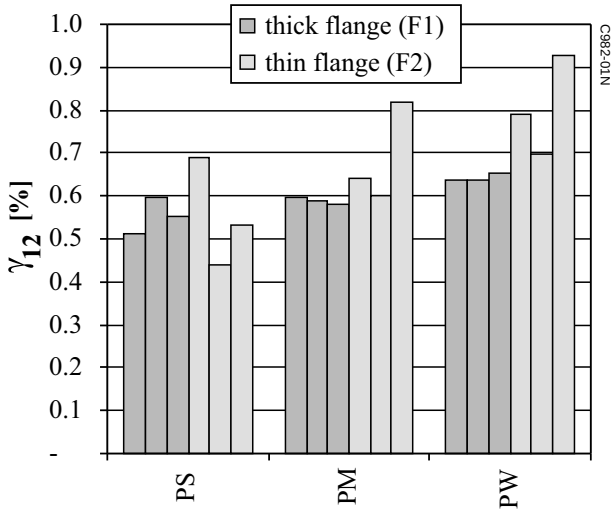

Fig. 6 Shear angle at failure for all specimens tested in four-point bending

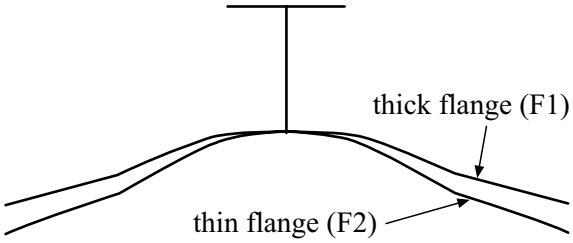

Fig 7 Deformation along the centre line calculated by finite element analysis for a load equal to the failure load

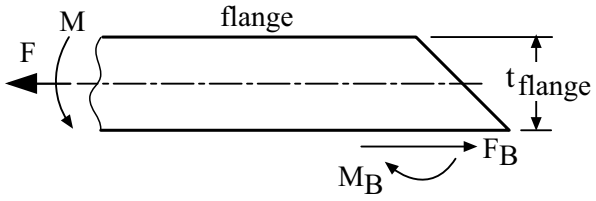

Fig 8 Cross section perpendicular to stringer direction of flange tip showing loads and moments acting on the flange

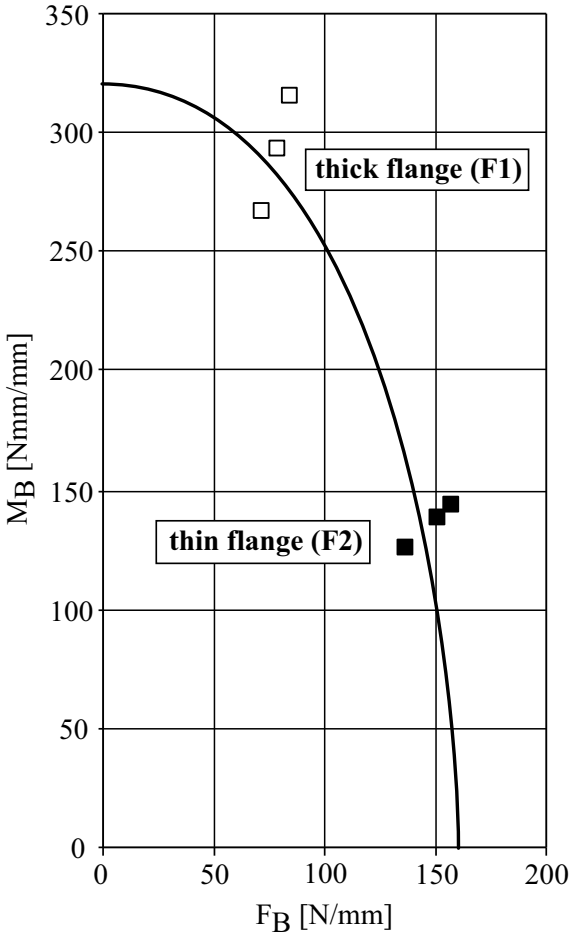

Fig 9 Shear load F_B and moment M_B transferred through the bond layer at failure

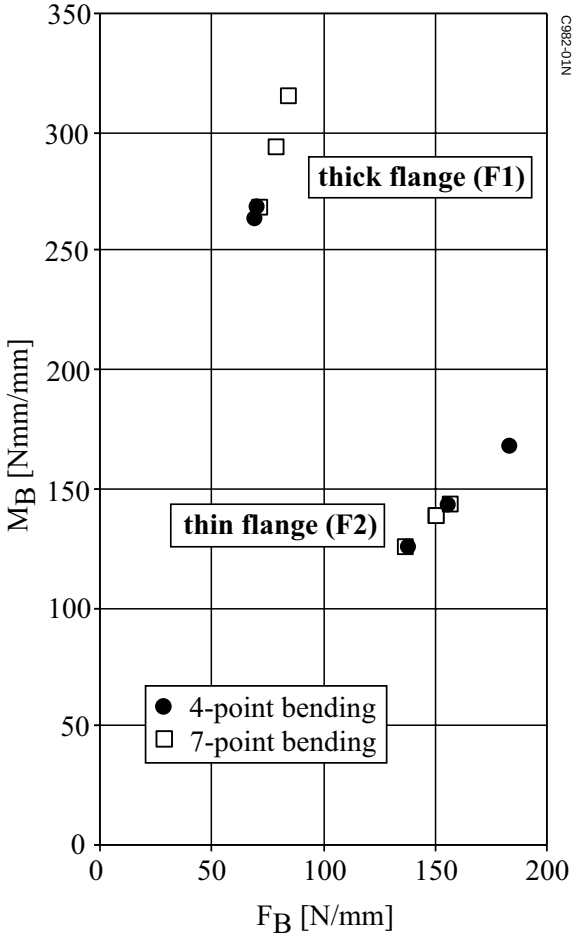

Fig 10 Shear load F_B and moment M_B transferred through the bond layer at failure for 100 mm specimens tested in four-point bending and specimens tested in seven-point bending